Development and Characterisation of Patch and Bowtie Antennae for Performance Investigation of Ground Penetrating Radar

Nairit Barkataki[1], Chandramita Bordoloi[1], Banty Tiru[2] and Utpal Sarma[1]
[1]Dept of Instrumentation & USIC, Gauhati University, Guwahati, India
[2]Dept of Physics, Gauhati University, Guwahati, India

***Abstract*—Ground penetrating radar (GPR) uses electromagnetic (EM) wave to detect the subsurface objects. Even though signal processing plays a significant role in GPR performance, the quality of the acquired data of a GPR system is significantly dependant on the antenna and transceiver electronics circuitry used. Bow-tie antennas are widely used in GPR applications because of their lightweight design, planar structure and ultra-wideband characteristics. Recent advances in planar microstrip antenna design has thrown up lots of possibilies for this antenna type in GPR applications. In this article, a comparative analysis of a planar microstrip antenna and a bow-tie slot antenna is presented. Both antennae are designed for a centre frequency of 1.5GHz and are fabricated on FR4 substrate. The planar microstrip antenna is fed with a 50 Ω microstrip line whereas the bow-tie antenna is fed with co-planar waveguide with 50 Ω impedance matching. The bow-tie antenna exhibits a return loss of $<$-10 dB across its measured bandwidth of $\sim$53%. On the other hand, the microstrip antenna exhibits a VSWR of 1.05 and return loss of -30.53 dB at its centre frequency of 1.5GHz.**

***Index Terms*—patch, bowtie, slot, antenna, ground penetrating radar**

I. Introduction

Ground Penetrating Radar (GPR) is used to detect subsurface objects with high resolution. Ground penetrating radar can be used to uncover hidden sources of disaster [1]. Consequently, it has been used in applications such as estimation of bridge state of deterioration [2], characterisation of mortar crack [3], soil surveys [4], pavement and sub-pavement structure diagnosis [5], bedrock identification [6], detection of cavities in fragile regions [7]. GPR can be used for investigation of tree root biomass which helps in soil amelioration, water infiltration, aeration through root channels and prevention of erosion [8]. In short, GPR has applications in a varied fields like environmental, archaeological, civil engineering, military, geophysical and so on [9].

In terms of power, the overall efficiency of a GPR system depends on the types of antennae used. The modelling, design and analysis of GPR antennae have to be done considering the fact that such systems have to be operated in close proximity to the subsurface media. The designers should take into account various characteristics like propagation path, media through which Radio Frequency (RF) wave propagates and the frequency & bandwidth of operation. The frequency of operation determines the penetration depth and bandwidth of operation determines resolution of the system.

Usually, such propagation media is lossy and heterogeneous in nature. The media acts as low pass filter which puts restrictions on using higher frequencies. Moreover, better resolution demands use of higher frequency. Simultaneously achieving a low frequency of operation for larger penetration depth and higher frequency for better resolution are mutually conflicting goals. Moreover, eliminating the effects of the propagation media on the higher frequencies of the antenna is also a challenge. Therefore, designers model and design the antenna keeping an optimal trade-off between the required penetration depth and resolution corresponding to the intended application.

Antenna Types for GPR

A high performance GPR system needs an antenna which has ultrawideband (UWB) characteristics, high gain and efficiency, low form factor and so on [10]. Hence, types of antennae which can meet such stringent demands are limited to Dipole antenna [11], Vivaldi antenna [12], TEM (transverse electromagnetic) horn antenna [10], [13]–[15], bowtie antenna [13], [16]–[19], planar spiral antenna [10], [13], and so on.

Most of the antenna types discussed above have wide bandwidth and simple structure. However, most of them are not suitable for fabrication using printed circuit boards as they do not have planar structures. Even if they have a planar structure, the problem of feeding and impedance matching arises as they cannot be printed on the same PCB as the one having associated electronics.

Planar Antenna

Planar antenna with microstrip or co-planar waveguide feeding is a suitable option for integration with PCB circuitry. In recent times, patch antenna [20], [21] is gaining popularity in GPR applications, given its low profile, lightweight, inexpensive and UWB characteristics.

There are many planar antenna designs, including planar metal-plate antenna [22], half-disk antenna [23] and planar horn antenna [24]. Several rectangular patch antenna designs have been reported in various literature. They have various configurations like circular, elliptical, square, pentagonal, hexagonal and so on which enhance their UWB characterictics

This work was supported by MeitY (Govt. of India) under Visvesvaraya PhD Scheme

[25], [26]. Half-square [27], semi-circular [28] and Half-hexagonal [29] monopole designs have also been reported for UWB applications. Patch antennae with quasi-transmission lines and band dispensation have been presented in [30], [31].

Feeding Mechanisms

Various feeding machanisms like microstrip line (MPL), coplanar waveguide line (CPW), coplanar parallel stripline, double sided parallel strip line and balun can be used to feed a planar antenna [32]. Among these, MPL and CPW are the most popular ones.

[33] shows the design and analysis of feeding techniques for microstrip lines. However, MPL have certain inherent disadvantages like narrow bandwidth and inability to feed balanced antennae like bow-tie, planar spiral etc. The cross sectional view of a microstrip line is shown in Fig. 1. Planar monopole antennae are generally fed with MPL as presented in [28], [34].

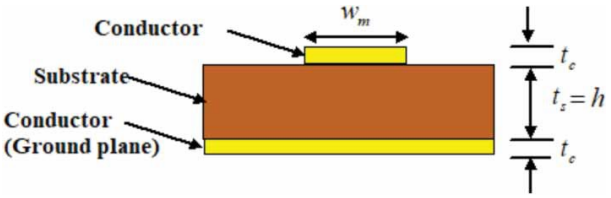

Fig. 1. A cross sectional view of MPL [32]

CPW is preferred for feeding antennae which have balanced output as well as various other advantages like ease of fabrication, control over impedance characteristics etc [35]. The cross sectional view of a coplanar waveguide is shown in Fig. 2. Wideband and balanced planar antennae are generally fed with CPW [24], [36], [37] as it retains the or enhances the wideband characteristics of the antennae and also helps in impedance matching. For antennae used in GPR applications, ungrounded CPW is generally used as the antenna side facing the earth's surface does not have any ground plane.

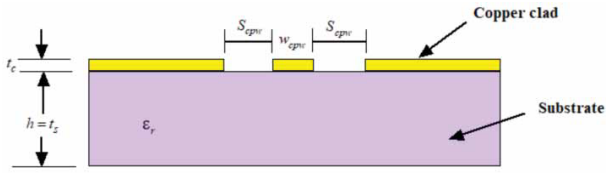

Fig. 2. A cross sectional view of CPW [32]

Aim of present work

In this paper, a comparative analysis of a planar microstrip antenna and a bow-tie slot antenna is presented. Both antennae are designed and simulated for a centre frequency of 1.5GHz and are fabricated on a FR4 substrate. The planar microstrip antenna is fed with a 50 Ω microstrip line whereas the bow-tie antenna is fed with a co-planar waveguide with 50 Ω impedance matching. The design parameters are optimised by multiple simulation runs. The antennae are finally fabricated on FR4 substrates and return loss measurements are obtained using a Rohde & Schwarz ZNB20 Vector Network Analyzer (VNA).

II. Antenna Design

A. Planar Microstrip Patch Antenna

A patch antenna consists of a radiating patch and either a full or partial ground plane. The partial ground plane can have a defected ground structure [38]. The electrical dimensions of the patch is a bit larger than its physical dimensions due to fringing effect. The difference between electrical and physical size also depends on the thickness and dielectric constant of the substrate (FR4 in this case).

The patch length is critical in design of the antenna as it determines the resonant frequency. The patch length L and width W for a rectangular patch antenna is given by [33] as:

$$L = \frac{c}{2f_r\sqrt{\epsilon_r}} \tag{1}$$

$$W = \frac{c}{2f_r\sqrt{\frac{(\epsilon_r+1)}{2}}} \tag{2}$$

where, c is the velocity of light, f_r is the resonant frequency and ϵ_r is the dielectric constant of the substrate.

The feed position of a patch antenna excited in its fundamental mode is typically located in the centre of the patch width and somewhere along the patch resonant length. The difference between electrical and physical size depends on fringing effect as well as the thickness and dielectric constant of the substrate (FR4 in this case).

The exact position along the resonant length is determined by the electromagnetic field distribution in the patch. Looking at the current (magnetic field) and voltage (electric field) variation along the patch, it is found that the the impedance is ∼50 Ω somewhere along the resonant length of the patch, around 12.5mm from the edge. This is the feeding point of the antenna. A microstrip line at the edge of the patch is used to feed it. The advantage of using MPL is the ability to place circuitry on the same PCB.

Impedance transformation to a useful value is needed as the impedance near the edge of the patch is quite high. This is solved by creating an inset for the microstrip line to the 50 Ω impedance point.

From equations 1 and 2, the length and width of the patch is calculated, considering f_r as 1.5Ghz and c = 3 $\times 10^8$ m/s.

The geometry of the proposed antenna is shown in Fig. 3. The antenna is designed on a double sided copper-clad FR4 substrate with a thickness of 1.6 mm and a permittivity of 4.3 and fed by a microstrip line. The thickness of copper clad is t_c = 0.035mm (1.4mils). The width of the microstrip feed line is fixed at 2.8 mm. The patch is backed by a ground plane, covering the entire area of the other side of the substrate. The dimensions are further optimised through several simulation runs to get the values as given in Table I

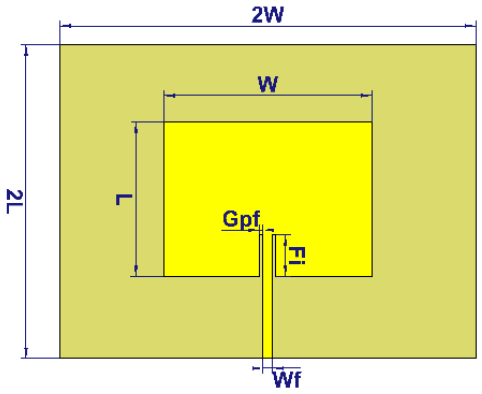

Fig. 3. Geometry of the microstrip antenna

TABLE I
OPTIMISED PARAMETERS FOR MPL FED PATCH ANTENNA DESIGN

Parameters	Symbols	Values
Length of the patch	L	45.65mm
Width of the patch	W	61.43mm
Length of the feed line	L_f	36.61mm
Width of the feed line	W_f	2.8mm
Height of the substrate, FR4	h	1.6 mm
Height of the conductor, Cu layer	t_c	0.035mm
Dielectric constant of the substrate	ϵ_r	4.3
Feed line inset length	F_i	12.5mm
Gap between feed line and patch	G_pf	1mm

B. CPW-fed Bow Tie Slot Antenna

Bow-tie antenna is a frequency-independent antenna as its characteristics are mainly specified by angles. The geometry, as shown in Fig. 4 of a bow-tie antenna is determined by three parameters [17]

- flare angle θ_0 affects the bandwidth
- gap distance **g** influences the antenna performance
- arm length **a** affects radiation efficiency

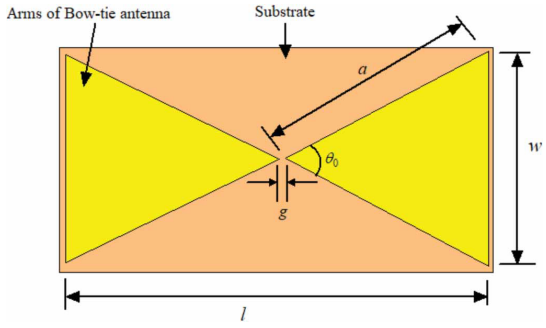

Fig. 4. Geometry of the microstrip antenna [32]

The characteristic impedance of the bow-tie antenna primarily depends upon the flaring angle and is given by [39] as

$$Z_c = 120 \ln\left(\cot\left(\frac{\theta_0}{4}\right) a\right) \tag{3}$$

where θ_0 is the opening angle of each side (also known as flare angle). The length l of the bow-tie antenna [40] is given by the following equation:

$$l = \lambda_0 \times \left(\frac{1}{\sqrt{\epsilon_{eff}}}\right) \tag{4}$$

where λ_0 is the wavelength corresponding to expected lowest operating frequency. The effective dielectric constant can be calculated by [32], [39]:

$$\epsilon_{eff} = \left(\frac{\epsilon_r + 1}{2}\right) + (\epsilon_r - 1)\left(1 + \left(10\frac{h}{w}\right)\right)^{-0.5555} \tag{5}$$

where w is the bow-tie antenna width in mm, h is the substrate thickness in mm, ϵ_r is the dielectric constant of the substrate.

A slot type structure is chosen for the bow-tie as it gives better control over its radiation pattern. The next task is to design a feed line with an impedance transformation from 50 Ω to 100 Ω. A coplanar waveguide feed is chosen for this purpose due to advantages like ease of fabrication and control over impedance characteristics.

The characteristic impedance, Z_0, of the ungrounded CPW line is calculated by the following equation as specified in [41]:

$$Z_0 = \left(\frac{30 \times \pi}{\sqrt{\epsilon_{eff}}}\right)\left(\frac{K(k')}{K(k)}\right) \tag{6}$$

where

$$\epsilon_{eff} = 1 + \left\{\frac{(\epsilon_r - 1)}{2}\right\}\left\{\left(\frac{K(k')}{K(k)}\right)\left(\frac{K(k_1)}{K(k_1')}\right)\right\} \tag{7}$$

$$k = \frac{w_{cpw}}{w_{cpw} + 2S_{cpw}} \tag{8}$$

$$k_1 = \frac{\sin h\left(\frac{\pi w_{cpw}}{4h}\right)}{\sin h\left(\frac{(w_{cpw} + 2S_{cpw})\pi}{4h}\right)} \tag{9}$$

$$k' = \sqrt{(1 + k^2)} \tag{10}$$

Here, k denotes complete elliptic integral of the first kind, w_{cpw} is the central strip width, S_{cpw} is the gap width of the CPW line and h is the height of the substrate, as shown in Fig. 2.

By using the Equations (3) to (10), the design parameters of the CPW line of characteristic impedance of 50 Ω and that of the bow-tie antenna are calculated.

The geometry of the proposed antenna is shown in Fig. 5. The antenna is designed on a single sided copper-clad FR4 substrate with a thickness of 1.6 mm and a permittivity of 4.3 and fed by a CPW line. The thickness of copper clad is t_c

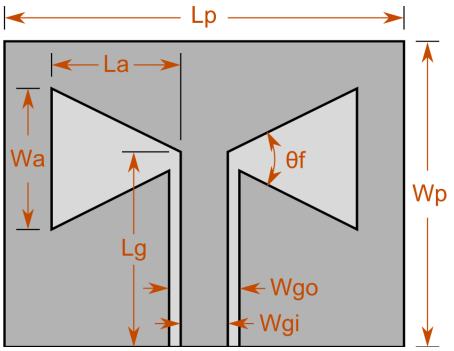

Fig. 5. Geometry of the bow-tie antenna

= 0.035mm (1.4mils). The dimensions are further optimised through several simulation runs to get the following final values as given in Table II.

TABLE II
OPTIMISED PARAMETERS FOR CPW FED BOWTIE ANTENNA DESIGN

Parameters	**Symbols**	**Values**
Arm Length	L_a	72.10mm
Arm width	W_a	42.50mm
Feeding angle	θ_f	31.88°
Length of CPW feed line	L_g	133.00mm
Inner width of the CPW feed line	W_{gi}	2.80mm
Outer width of the CPW feed line	W_{go}	3.80mm
Length of the substrate, FR4	L_p	180.00 mm
Width of the substrate, FR4	W_p	170.00 mm
Height of the substrate, FR4	h	1.6 mm
Height of the conductor, Cu layer	t_c	0.035mm
Dielectric constant of the substrate	ϵ_r	4.3

III. Results and Discussion

A. Return Loss and VSWR

The microstrip antenna is excited with 50 Ω waveguide port and simulated. The antenna is later fabricated on a FR4 substrate conforming to the simulated deign and return loss & VSWR are measured with a Rohde & Schwarz ZNB20 Vector Network Analyzer (VNA). Figures 6 and 7 show the simulated and experimental return loss and VSWR characteristics of the microstrip patch antenna.

As seen from the figures, simulated results closely resemble the measured results. The simulated bandwidth covers from 1.48 GHz to 1.52 GHz (∼2.66%) at S11 = -10dB level with minimum return loss at 1.50 GHz (-29.33 dB), while the measured bandwidth covers from 1.494 GHz to 1.524 GHz (∼2%) with minimum return loss at 1.51 GHz (-30.53 dB). The slight discrepancies between the simulated and measured results may be attributed to the connector, which is not considered during simulation.

The CPW fed bowtie antenna is excited with 50 Ω waveguide port and simulated. The antenna is later fabricated on a FR4 substrate conforming to the simulated deign and return loss & VSWR are measured with a Rohde & Schwarz ZNB20 Vector Network Analyzer (VNA). Figures 8 and 9 show the simulated and experimental return loss and VSWR characteristics of the microstrip patch antenna.

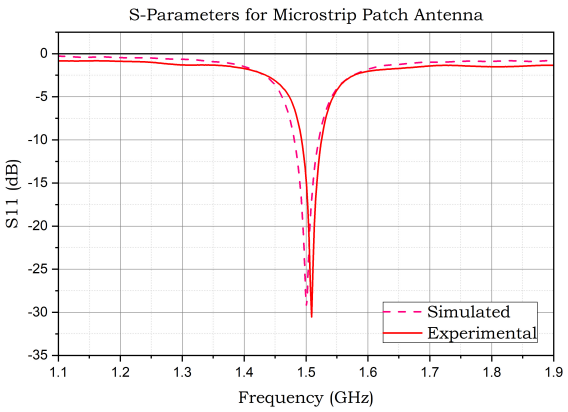

Fig. 6. S-Parameters of Microstrip Patch Antenna

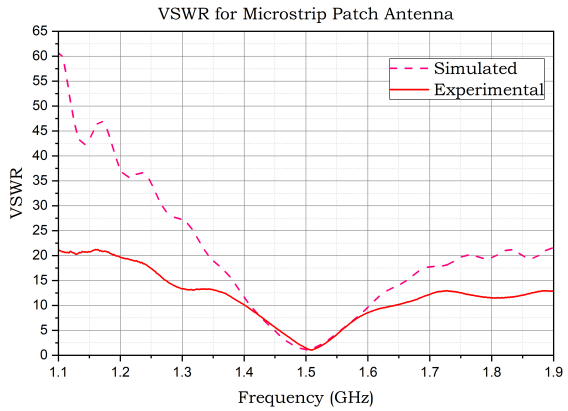

Fig. 7. VSWR of Microstrip Patch Antenna

As seen from the figures, the simulated bandwidth covers from 1.33 GHz to 1.96 GHz (42%) at S11 = -10dB level with minimum return loss at 1.499 GHz (-36.99), while the measured bandwidth covers from 1.36 GHz to 2.15 GHz (∼52.67%) with minimum return loss at 1.55 GHz (-18.29). The discrepancies between the simulated and measured results may be attributed to the connector used, which is not considered during simulation and defects during fabrication of the CPW feed line. The measured results show a better bandwidth (∼52.67%) than the simulated results (42%). it is seen that the bowtie antenna has a much better bandwidth than the microstrip antenna for the same centre frequency of 1.5 GHz.

B. Radiation Pattern

Figures 10 and 11 show the simulated 3D radiation patterns of the microstrip and bowtie antennae. It is seen that the microstrip antenna has a maximum gain of 1.57dB whereas

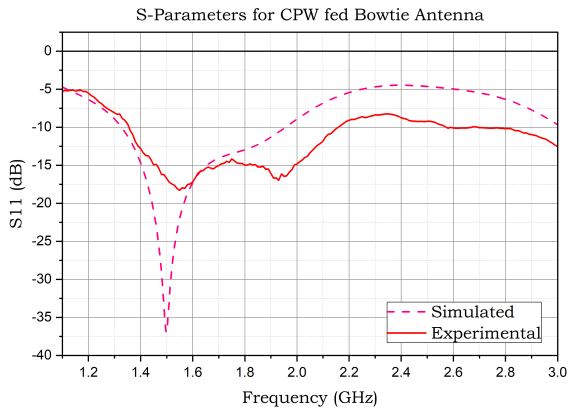

Fig. 8. S-Parameters of Bowtie Antenna

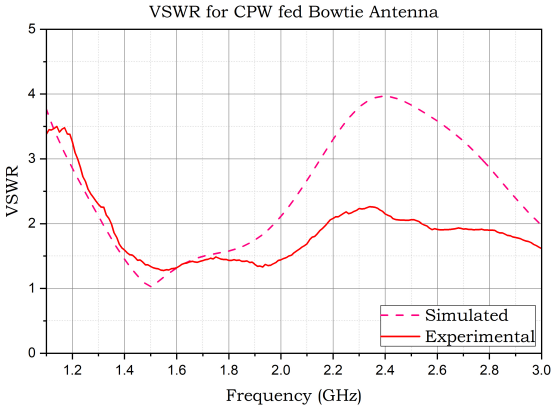

Fig. 9. VSWR of Bowtie Antenna

the bowtie antenna has a maximum gain of 7.02 dB. The higher gain of the bowtie will definitely make it a better GPR antenna because the signal can propagate deeper under the ground surface.

IV. Summary

In this paper, simulated and measurement results of a planar microstrip antenna and a bow-tie slot antenna are discussed. The use of UWB signal source in GPR is well known. The main advantage of using a UWB signal is the need for better vertical resolution (depth resolution). The measured bandwidth of the bowtie antenna is ∼52.67% (1.36 GHz to 2.15 GHz) as compared to the microstrip antenna's bandwidth of ∼2% (1.494 GHz to 1.524 GHz). The microstrip antenna has a maximum gain of 1.57dB whereas the bowtie antenna has a maximum gain of 7.02 dB. The higher bandwidth and gain of the bowtie antenna makes it a better GPR antenna with deep penetration and better resolution imaging. It's planar structure, low form factor and lightweight design makes the bowtie antenna easy to be integrated within the enclosure containing the other GPR equipments, as compared to other antenna types

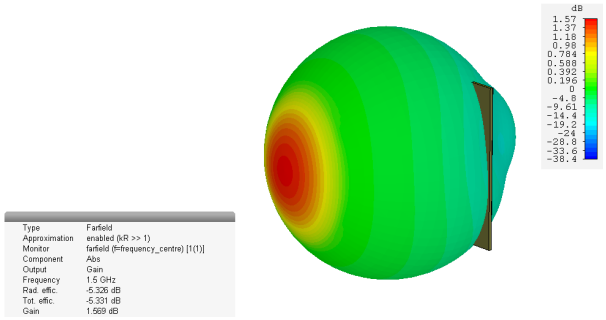

Fig. 10. Radiation pattern of Microstrip Patch Antenna at 1.5 GHz

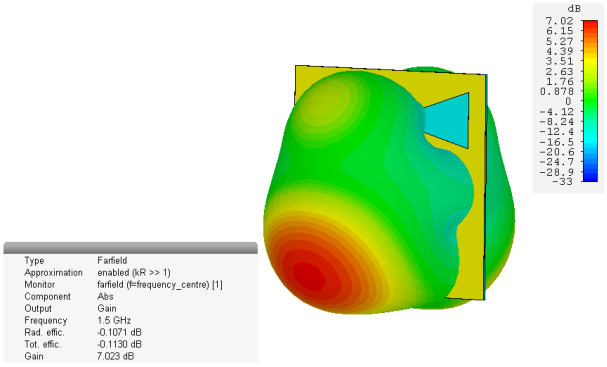

Fig. 11. Radiation pattern of Bowtie Antenna at 1.5 GHz

such as horn, spiral etc. The CPW feeding mechanism makes the bowtie antenna suitable for integration with PCB circuitry.

The GPR waveform is usually a short pulse with a very large instantaneous bandwidth. Such short pulses are generated by imposing a step function voltage onto an antenna which creates a ringing effect (oscillations) for normal antennae. This phenomena is partially responsible for the masking of the buried targets in a GPR survey. By applying resistive loading to the antenna, this effect can be reduced. The authors plan to further improve the existing design by reducing the ringing effect.

Acknowledgement

The authors would like to thank the Ministry of Electronics and Information Technology (Govt. of India) for the financial support for this research work. The authors would also like to thank the Department of Electronics and Communication Technology (Gauhati University) for providing the equipment needed for carrying out the measurement for the fabricated antennae.

References

[1] X. Xu, S. Peng, and F. Yang, "Development of a ground penetrating radar system for large-depth disaster detection in coal mine," *Journal of Applied Geophysics*, vol. 158, pp. 41 – 47, 2018.

[2] M. Alsharqawi, T. Zayed, and S. A. Dabous, "Integrated condition rating and forecasting method for bridge decks using visual inspection and ground penetrating radar," *Automation in Construction*, vol. 89, pp. 135 – 145, 2018.

[3] C. W. Chang, C. H. Lin, and Q.-W. Yuan, "Quantitative study of electromagnetic wave characteristic values for mortars crack," *Construction and Building Materials*, vol. 175, pp. 351 – 359, 2018.

[4] K. Zajcov and T. Chuman, "Application of ground penetrating radar methods in soil studies: A review," *Geoderma*, vol. 343, pp. 116 – 129, 2019.

[5] A. Benedetto, F. Benedetto, and F. Tosti, "Gpr applications for geotechnical stability of transportation infrastructures," *Nondestructive Testing and Evaluation*, vol. 27, no. 3, pp. 253–262, 2012.

[6] M. C. Diallo, L. Z. Cheng, E. Rosa, C. Gunther, and M. Chouteau, "Integrated gpr and ert data interpretation for bedrock identification at clricy, qubec, canada," *Engineering Geology*, vol. 248, pp. 230 – 241, 2019.

[7] G. Alsharahi, A. Faize, M. Louzazni, A. Mostapha, M. Bayjja, and A. Driouach, "Detection of cavities and fragile areas by numerical methods and gpr application," *Journal of Applied Geophysics*, vol. 164, pp. 225 – 236, 2019.

[8] K. A. Borden, M. E. Isaac, N. V. Thevathasan, A. M. Gordon, and S. C. Thomas, "Estimating coarse root biomass with ground penetrating radar in a tree-based intercropping system," *Agroforestry systems*, vol. 88, no. 4, pp. 657–669, 2014.

[9] H. M. Jol, *Ground penetrating radar theory and applications*. elsevier, 2008.

[10] D. J. Daniels, *Ground penetrating radar*. The Institution of Electrical Engineers, 2004.

[11] E. Ávila-Navarro, J. A. Carrasco, and C. Reig, "Printed dipole antennas for personal communication systems," *IETE Technical Review*, vol. 27, no. 4, pp. 286–292, 2010.

[12] W. Wiesbeck, G. Adamiuk, and C. Sturm, "Basic properties and design principles of uwb antennas," *Proceedings of the IEEE*, vol. 97, no. 2, pp. 372–385, 2009.

[13] I. Hertl and M. Strycek, "Uwb antennas for ground penetrating radar application," in *2007 19th International Conference on Applied Electromagnetics and Communications*. IEEE, 2007, pp. 1–4.

[14] A. A. Jamali and R. Marklein, "Design and optimization of ultra-wideband tem horn antennas for gpr applications," in *2011 XXXth URSI General Assembly and Scientific Symposium*. IEEE, 2011, pp. 1–4.

[15] H. A. Mohamed, H. Elsadek, and E. A. Abdallah, "Quad ridged uwb tem horn antenna for gpr applications," in *2014 IEEE Radar Conference*. IEEE, 2014, pp. 0079–0082.

[16] A. S. Turk, D. A. Sahinkaya, M. Sezgin, and H. Nazli, "Investigation of convenient antenna designs for ultra-wide band gpr systems," in *2007 4th International Workshop on, Advanced Ground Penetrating Radar*. IEEE, 2007, pp. 192–196.

[17] J. Wang, Y. Su, C. Huang, M. Lu, and Y. Li, "Design of bow-tie antenna with high radiating efficiency for impulse gpr," in *2012 IEEE International Geoscience and Remote Sensing Symposium*. IEEE, 2012, pp. 594–597.

[18] K. Ajith and A. Bhattacharya, "Improved ultra-wide bandwidth bow-tie antenna with metamaterial lens for gpr applications," in *Proceedings of the 15th International Conference on Ground Penetrating Radar*. IEEE, 2014, pp. 739–744.

[19] R. Nayak, S. Maiti, and S. K. Patra, "Design and simulation of compact uwb bow-tie antenna with reduced end-fire reflections for gpr applications," in *2016 International Conference on Wireless Communications, Signal Processing and Networking (WiSPNET)*. IEEE, 2016, pp. 1786–1790.

[20] A. Z. Alam, M. R. Islam, and S. Khan, "Design and analysis of uwb rectangular patch antenna," in *2007 Asia-Pacific Conference on Applied Electromagnetics*. IEEE, 2007, pp. 1–3.

[21] M. Karim, M. Malek, M. Jamlos, and N. Saudin, "Ground penetrating radar: Antenna for buried object detection," in *2013 IEEE Symposium on Wireless Technology & Applications (ISWTA)*. IEEE, 2013, pp. 198–201.

[22] K.-L. Wong, C.-H. Wu, and S.-W. Su, "Ultrawide-band square planar metal-plate monopole antenna with a trident-shaped feeding strip," *IEEE Transactions on Antennas and Propagation*, vol. 53, no. 4, pp. 1262–1269, 2005.

[23] T. Yang and W. A. Davis, "Planar half-disk antenna structures for ultra-wideband communications," in *IEEE Antennas and Propagation Society Symposium, 2004.*, vol. 3. IEEE, 2004, pp. 2508–2511.

[24] S. H. Lee, J. K. Park, and J. N. Lee, "A novel cpw-fed ultra-wideband antenna design," *Microwave and Optical Technology Letters*, vol. 44, no. 5, pp. 393–396, 2005.

[25] S.-W. Su, K.-L. Wong, and C.-L. Tang, "Ultra-wideband square planar monopole antenna for ieee 802.16 a operation in the 2–11-ghz band," *Microwave and optical technology letters*, vol. 42, no. 6, pp. 463–466, 2004.

[26] J. Jung, W. Choi, and J. Choi, "A small wideband microstrip-fed monopole antenna," *IEEE microwave and wireless components letters*, vol. 15, no. 10, pp. 703–705, 2005.

[27] M. G. N. Alsath and M. Kanagasabai, "Compact uwb monopole antenna for automotive communications," *IEEE Transactions on Antennas and Propagation*, vol. 63, no. 9, pp. 4204–4208, 2015.

[28] P. Jain, B. Singh, S. Yadav, and A. Verma, "A semicircular monopole antenna for ultra-wideband applications," in *Proceedings of International Conference on ICT for Sustainable Development*. Springer, 2016, pp. 339–345.

[29] U. Keshwala, S. Rawat, and K. Ray, "Compact half-hexagonal monopole planar antenna for uwb applications," in *Soft Computing: Theories and Applications*. Springer, 2018, pp. 225–231.

[30] C.-W. Ling and S.-J. Chung, "A simple printed ultrawideband antenna with a quasi-transmission line section," *IEEE Transactions on Antennas and Propagation*, vol. 57, no. 10, pp. 3333–3336, 2009.

[31] K. G. Thomas and M. Sreenivasan, "A simple ultrawideband planar rectangular printed antenna with band dispensation," *IEEE Transactions on antennas and propagation*, vol. 58, no. 1, pp. 27–34, 2009.

[32] R. Nayak and S. Maiti, "A review of bow-tie antennas for gpr applications," *IETE Technical Review*, pp. 1–16, 2018.

[33] R. Garg, P. Bhartia, I. J. Bahl, and A. Ittipiboon, *Microstrip antenna design handbook*. Artech house, 2001.

[34] M. N. Shakib, M. Moghavvemi, and W. N. L. Mahadi, "Design of a compact planar antenna for ultra-wideband operation," *Applied Computational Electromagnetics Society Journal*, vol. 30, no. 2, pp. 222–229, 2015.

[35] H. J. Visser, *Antenna theory and applications*. John Wiley & Sons, 2012.

[36] M. Karim, M. Malek, M. Jamlos, A. Abdullah, N. M. Noorpi, N. Mokhtar, and M. Jusoh, "Cpw circular patch antenna for ground penetrating radar applications," in *Theory and Applications of Applied Electromagnetics*. Springer, 2015, pp. 59–67.

[37] S. M. H. Varkiani and M. Afsahi, "Compact and ultra-wideband cpw-fed square slot antenna for wearable applications," *AEU-International Journal of Electronics and Communications*, vol. 106, pp. 108–115, 2019.

[38] D. M. Elsheakh and E. A. Abdallah, "Novel shapes of vivaldi antenna for ground pentrating radar (gpr)," in *2013 7th European Conference on Antennas and Propagation (EuCAP)*. IEEE, 2013, pp. 2886–2889.

[39] M. Rahim, M. A. Aziz, and C. Goh, "Bow-tie microstrip antenna design," in *2005 13th IEEE International Conference on Networks Jointly held with the 2005 IEEE 7th Malaysia International Conf on Communic*, vol. 1. IEEE, 2005, pp. 4–pp.

[40] G. Chen and R. C. Liu, "A 900mhz shielded bow-tie antenna system for ground penetrating radar," in *Proceedings of the XIII Internarional Conference on Ground Penetrating Radar*. IEEE, 2010, pp. 1–6.

[41] G. Ghione and C. Naldi, "Analytical formulas for coplanar lines in hybrid and monolithic mics," *Electronics Letters*, vol. 20, no. 4, pp. 179–181, 1984.